Catalysis Today 153 (2010) 103–110

Contents lists available at ScienceDirect

Catalysis Today

journal homepage: www.elsevier.com/locate/cattod

Characteristics of low platinum Pt–BaO catalysts for NO_x storage and reduction

Wei-Zhen Li, Ke-Qiang Sun*, Zhun Hu, Bo-Qing Xu*

Innovative Catalysis Program, Key Lab of Organic Optoelectronics and Molecular Engineering, Department of Chemistry, Tsinghua University, Beijing 100084, China

ARTICLE INFO

Article history:
Available online 2 April 2010

Keywords:
NO_x storage and reduction
Low platinum catalysts
Pt–BaO catalysts
N_2 selectivity
Cobalt oxides
ZrO_2–Al_2O_3

ABSTRACT

The characteristics of low platinum Pt–BaO catalysts for NO_x storage and reduction (NSR) were studied over three series of samples that have similar barium loadings (ca. 15 wt% Ba), namely, Pt–BaO/Al_2O_3, CoO_x promoted Pt–BaO/Al_2O_3 and Pt–BaO/ZrO_2–Al_2O_3 catalysts. The catalysts were calcined at 800 °C and their NSR performances were evaluated under cyclic lean (1000 ppm NO and 10 vol% O_2 in Ar)/rich (1 vol% H_2 in Ar) conditions with particular attention paid to detect the possible harmful by-products, i.e., NH_3 and N_2O, during the reduction of the stored NO_x under the rich condition. Lowering the Pt loading in the Pt–BaO/Al_2O_3 catalyst from 1.0 to 0.5 wt% resulted in a 15% decrease in the NO_x storage capacity (NSC) under the lean condition but the N_2 selectivity under the rich condition declined dramatically (from 85% to 53%), indicating that the NO_x reduction performance under the rich condition is the key to low platinum NSR catalysts. The cobalt oxides was identified as an unsuitable promoter for lowering the Pt loading; its addition into Pt–BaO/Al_2O_3 at the Pt loading of 0.5 wt% further reduced the N_2 selectivity under the rich condition although significant improvement in the NSC under lean condition could be observed. It was found instead that the use of ZrO_2–Al_2O_3 as an alternative of the Al_2O_3 support was effective in lowering the dependence on Pt loading of the Pt–BaO for the NSR catalysis since the ZrO_2–Al_2O_3 support could make the catalyst highly selective for the formation of N_2 under the rich condition, at a lower Pt loading. The overall NSR performance of a Pt–BaO/ZrO_2–Al_2O_3 catalyst with 0.5 wt% Pt was found comparable to that of its counterpart Pt–BaO/Al_2O_3 catalyst with 1.0 wt% Pt, demonstrating a viable way for developing low platinum NSR catalysts.

1. Introduction

Automobile lean-burn engines (air/fuel ratio >22) can improve fuel efficiency as high as 20–30% over the traditional stoichiometric engines (air/fuel ratio = 14.7), and in turn can significantly reduce CO_2 emission. However, the currently widely used three-way catalytic converters have been optimized for the stoichiometric engines and are ineffective for NO_x abatement due to the presence of excess oxygen in the lean exhausts. Development of new catalytic system capable of reducing NO_x to N_2 in the oxygen-rich exhausts has since remained as an obstacle to the emission control for such fuel efficient automobiles [1].

The catalytic NO_x storage and reduction (NSR) or lean NO_x trap (LNT) technology, proposed by Toyota researchers in the middle of 1990s [2,3], has been recognized as one of the most promising solutions for lean NO_x abatement. The principle of NSR technology is based on the storage of NO_x primarily as nitrates over a NSR catalyst under the normal lean-burn operation (lean storage phase), and then reduction of the stored nitrates to N_2 by intermittently switching the engine to a short rich operation which recovers the NO_x storage capacity of the catalyst (rich regeneration phase). To fulfill these functions, a NSR catalyst is therefore composed of precious metals (typically Pt) for oxidation and reduction reactions, alkali or alkaline earth metal oxides (commonly BaO) for NO_x trapping, using usually Al_2O_3 as the support [1–5]. However, the current NSR technology is quite expensive, i.e., the loadings of precious metals are nearly doubled as compared with those in the traditional three-way converters [6]. This is because NSR catalysts would undergo severe deactivation due to the unavoidable formation of poisonous $BaSO_4$ from sulfur-containing contaminates and/or hot spots generated during rich engine operations. In fact these two origins could be essentially ascribed to thermal deactivation since the catalyst recovery by desulfation would also require high temperature operations (ca. >650 °C) [3–5]. Thus, the development of a practical NSR catalyst would have to meet with the two challenges, namely, improving the catalyst resistance to thermal sintering (thermal stability) and lowering the dependence on precious metals without sacrificing the NO_x storage-reduction capabilities.

Great efforts have been devoted to improve the NO_x storage and reduction performance on supported Pt–BaO catalysts. Using more acidic oxides (e.g., TiO_2–ZrO_2) as support [3,7,8] or promoting with transition metal oxides [5] could effectively improve their sulfur-resistance ability. Recently it was discovered that promot-

* Corresponding authors. Tel.: +86 10 62792122; fax: +86 10 62792122.
E-mail addresses: kqsun@mail.tsinghua.edu.cn (K.-Q. Sun), bqxu@mail.tsinghua.edu.cn (B.-Q. Xu).

0920-5861/$ – see front matter © 2010 Elsevier B.V. All rights reserved.
doi:10.1016/j.cattod.2010.02.056

ing Pt–BaO/Al_2O_3 with cobalt oxides could greatly increase the NO_x storage capacity (NSC) [9]. CeO_x [10] and MnO_x [11] were reported to produce similar promotional effects. These results suggest that using in-expensive transition metal oxides would be a promising approach in the search for low Pt NSR catalysts. However, studies in the open literature were mainly dedicated to the discussion of the NO_x storage performance under lean conditions, little study was made to investigate the performance of the promoted catalysts in the regeneration phase or under rich conditions. In fact the regeneration phase is most demanding since in the short regeneration phase the catalyst must reduce to nonpoisonous N_2 a large amount of NO_x accumulated during the long storage phase. However, the possible formation of harmful by-products, such as NH_3 and N_2O, as have been detected in a few recent documentations [11–15], was usually not determined. Knowledge about the NO_x reduction performance of low platinum Pt–Ba/Al_2O_3 is thus very limited in the literature.

In the first part of this present study, the reduction catalysis of CoO_x promoted Pt–BaO/Al_2O_3 catalysts is investigated in relation with their catalysis for the lean NO_x storage. The second part of this study would demonstrate that using ZrO_2–Al_2O_3 as an alternative of the Al_2O_3 support can lower the dependence on Pt of the Pt–BaO catalyst. High temperature (800 °C) calcination and reduction pretreatment were applied in this work to better approach the performance of thermally aged Pt–BaO NSR catalyst since thermal deactivation was identified as one of the main origins affecting the stability of a practical NSR catalyst [3–5]. Particular attention is paid to detect formation of poisonous NH_3 and N_2O during the reduction of the stored NO_x under rich condition.

2. Experimental

2.1. Sample preparation

2.1.1. Preparation of Al_2O_3 and ZrO_2–Al_2O_3

The γ-Al_2O_3 support (S_{BET} = 160 m^2/g, pore volume Vp = 0.37 cm^3/g) was prepared through conventional hydrolysis of $Al(NO_3)_3{\cdot}9H_2O$ with aqueous ammonia solution at pH 10. The obtained $Al(OH)_3$ hydrogel was then thoroughly washed, dried at 110 °C overnight and calcined in flowing air at 800 °C for 5 h.

The ZrO_2–Al_2O_3 composite oxide was prepared by a sequential two-step hydrolysis method, namely, the hydrolysis of the $Al(NO_3)_3{\cdot}9H_2O$ solution was followed by a hydrolysis of $ZrO(NO_3)_2{\cdot}2H_2O$ in aqueous ammonia solution at pH 10. The obtained $ZrO(OH)_2$–$Al(OH)_3$ hydrogel was then washed, dried and then calcined with the procedures used for preparing the γ-Al_2O_3 support as mentioned above. The weight percentage of ZrO_2 in ZrO_2–Al_2O_3 determined by XRF analysis was 10 wt%.

2.1.2. Preparation of Pt–BaO/Al_2O_3, Pt–CoO_x–BaO/Al_2O_3 and Pt–BaO/ZrO_2–Al_2O_3 catalysts

Pt–BaO/Al_2O_3, Pt–CoO_x–BaO/Al_2O_3 and Pt–BaO/ZrO_2–Al_2O_3 catalysts with similar barium loadings (ca. 15 wt% Ba) were prepared via a sequential two-step wet impregnation method. In the first step, BaO/Al_2O_3 and BaO/ZrO_2–Al_2O_3 were prepared, respectively, by wet impregnation of the γ-Al_2O_3 and ZrO_2–Al_2O_3 supports with an aqueous solution of $Ba(NO_3)_2$, followed by drying at 60 °C in a rotary evaporator and calcination in flowing air at 800 °C for 5 h. In the second step, Pt was loaded on to the prepared BaO/Al_2O_3 and BaO/ZrO_2–Al_2O_3 samples by impregnation with an aqueous solution of $Pt(NH_3)_4(NO_3)_2$ to prepare the Pt–BaO/Al_2O_3 and Pt–BaO/ZrO_2–Al_2O_3, respectively. The Pt–CoO_x–BaO/Al_2O_3 catalysts were prepared by co-impregnation of BaO/Al_2O_3 with an aqueous solution of $Pt(NH_3)_4(NO_3)_2$ (Alfa) and $Co(NO_3)_2{\cdot}6H_2O$, followed by drying at 60 °C in a rotary evaporator and calcination in air flow at 800 °C for 5 h. These catalysts were denoted as *m*Pt–*n*CoO_x–BaO/support, where "*m*" and "*n*" represent, respectively, the Pt and Co loadings determined by XRF analysis.

2.2. Characterizations

BET surface areas of the samples were measured using the nitrogen adsorption–desorption isotherms at −196 °C on a Micromeritics ASAP 2010C instrument. Before the measurements the samples were degassed at 200 °C for 1 h.

X-ray diffraction (XRD) patterns were obtained on a Bruker D8 Advance X-ray diffractometer with a Ni-filtered Cu K_α (λ = 0.15406 nm) radiation source at 40 kV and 40 mA. The average crystallite sizes were calculated according to the well-known Scherrer equation, $D = 0.90\lambda/\beta\cos\theta$, where θ is the diffraction angle and β the full width at the half-maximum (FWHM).

The Pt dispersion was determined by H_2–O_2 titration experiment performed at 90 °C on a catalyst analyzer (BEL-A, Japan) with a mass spectrometer (Inprocess Instruments, GAM 200) as the detector. The sample load was normalized to have ca. 3 mg Pt for the measurement. And, prereduction of the samples was done at 800 °C for 0.5 h in a flow of 5% H_2 in Ar (30 mL/min), followed by lowering the reactor temperature to 90 °C in the same gas flow. The pre-oxidation of the sample was performed at 90 °C in a flow of 20% O_2 in Ar for 15 min. After an Ar purge, successive H_2 pulses were then admitted to measure the H_2 consumption data, which was then used to calculate the Pt dispersion according to the stoichiometries:

$$2Pt_s + O_2 \rightarrow 2Pt_s{-}O$$

$$2Pt_s{-}O + 3H_2 \rightarrow 2Pt_s{-}H + 2H_2O$$

where Pt_s denotes a surface Pt site.

H_2 temperature programmed reduction (H_2-TPR) was conducted on a home-made equipment with a TCD detector in a flow of 5% H_2 in Ar as described previously [16]. The temperature ramp was 10 °C/min and the H_2 consumption was calibrated by measuring the reduction of known amount of ultra high purity CuO.

2.3. Evaluation of NSR performance

The NSR performance of the catalysts was evaluated using a fixed bed quasi-plug-flow quartz reactor (4 mm i.d.) under cycling lean (1000 ppm NO and 10 vol% O_2 in Ar, 50 min) and rich (1 vol% H_2 in Ar, 15 min) conditions at 300 °C, with an Ar purge of 5 min intervened between the lean/rich switches. The Ar purge removes those NO_x reversibly adsorbed on the catalyst and flushes gaseous NO_x in the reactor tube, and thus avoids the mixing of the un-stored gaseous NO_x with the reductants introduced (hydrogen in this work) during the lean/rich switches, which decouples the selective catalytic reduction (SCR) performance of the NSR catalysts from their intrinsic performance for the reduction of the stored NO_x, since the Pt–BaO/Al_2O_3 NSR catalysts were found also active for the SCR reaction [12,13]. Prior to each test, the catalyst (60 mg) was pretreated in 5% H_2 in Ar at 800 °C for 30 min and subsequently cooled to 300 °C. The results presented in the present work were collected under cycle-average steady state which was generally achieved after the second or third cycle. The overall gas flow rate was 40 mL/min, which corresponds to a gas hourly space velocity of 40,000 mL g^{-1} h^{-1}. The reactor effluent was on-line analyzed by a well-calibrated mass spectrometer (Inprocess Instruments, GAM 200) with the following mass-to-charge (*m*/*e*) ratios: 2 (H_2), 15 (NH_3), 28(N_2), 30 (NO and NO_2), 32 (O_2), 40 (Ar), 44 (N_2O) and 46 (NO_2). The time-averaged product selectivity under the rich condition was calculated based on the numbers of nitrogen atoms in every N-containing species.

Temperature programmed desorption of NO_x (NO_x-TPD) and O_2 (O_2-TPD) experiments were conducted with the same setup for the NSR measurements in an Ar flow (40 mL/min) from room temperature (RT) to 800 °C with a ramp of 10 °C/min. Before the start of the NO_x-TPD measurement, the sample was saturated with NO_x in the cycle-average steady state under the lean condition. In the case of O_2-TPD, the sample was pretreated with a flowing gas containing 20% O_2 in Ar at 800 °C for 30 min to completely remove a possible catalyst contamination by carbonates. The sample was switched to an Ar flow after cooling to RT and was purged to have a stabilized background before recording the O_2-TPD profile.

3. Results and discussion

3.1. Catalyst characterization

Table 1 shows the composition, BET surface area and Pt dispersion of the Pt–BaO/Al_2O_3, Pt–CoO_x–BaO/Al_2O_3 and Pt–BaO/ZrO_2–Al_2O_3 catalysts. All of the catalysts had similar barium loadings (ca. 15 wt%). The Pt–BaO/Al_2O_3 and Pt–BaO/ZrO_2–Al_2O_3 showed similar specific BET areas (ca. 120 m^2/g). The surface area of Pt–CoO_x–BaO/Al_2O_3 decreased from 109 to 69 m^2/g when cobalt loading was increased from 1 to 10 wt%. The Pt dispersions measured from the H_2–O_2 titration measurements and evaluated using the average Pt sizes obtained according to Scherer equation based on the diffraction of metallic platinum at $2\theta = 39.8°$ appeared quite similar, ca. 3.0%, and increased slightly with decreasing Pt loading. These Pt dispersion data are comparable to those of thermally aged catalysts [4,17] but much lower than those (20–80%) of catalysts prepared typically with much lower calcination temperatures (usually 500 °C) [4,5,18] since the present catalysts were intentionally calcined using a temperature as high as 800 °C to better approach the performance of thermally aged Pt–BaO NSR catalyst.

3.2. Effect of Pt loading on NSR performance of Pt–BaO/Al_2O_3

Fig. 1 shows the time-course of NO_x storage under the lean condition (breakthrough curve) over Pt–BaO/Al_2O_3 catalysts. Upon admitting the mixture of NO and O_2 to the reactor, there was a short dead time before the simultaneously evolution of NO and NO_2, which suggests the complete adsorption of NO_x at the initial stage of NO_x storage. The outlet NO_x ($NO + NO_2$) concentration then increased gradually, and finally approached the inlet NO concentration (1000 ppm) after NO_x storage for over 25 min, which suggests the saturation of the catalysts with NO_x. Lowering the Pt loading from 1 to 0.1 wt% shortened significantly the dead time, and led to steeper NO curves after the breakthrough, The slopes of NO_2 curves

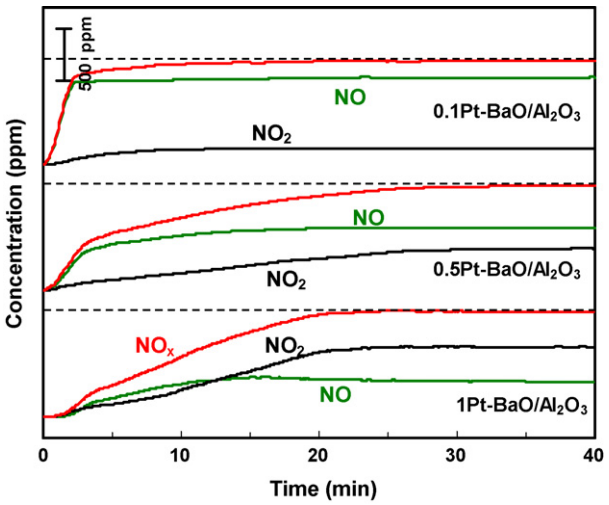

Fig. 1. Time-course of NO_x storage under the lean condition (breakthrough curve) over Pt–BaO/Al_2O_3 catalysts with Pt loading of 1.0, 0.5 and 0.1 wt%, respectively.

were less dependent on Pt loading, however, its concentration, after catalyst being saturated with NO_x, decreased obviously on lowering the Pt loading. This indicates that lowering the Pt loading decreases the oxidizing ability of the catalysts. The NSCs were then obtained from the breakthrough curves. 1Pt–BaO/Al_2O_3 showed a NSC of around 0.27 mmol/g-cat (Table 2), which is comparable to those measured under prolonged lean conditions where catalysts were nearly saturated with NO_x [9,19,20]. The NSC dropped by about 15% when the Pt loading was lowered from 1.0 to 0.5 wt%, and by 40% on further reducing the Pt loading from 0.5 to 0.1 wt%.

Two main mechanisms for NO_x storage have been proposed [4,5]: "nitrite route" – NO is oxidatively adsorbed as nitrites, followed by further oxidation of the nitrites to nitrates; and "nitrate route" – NO is oxidized to NO_2 on Pt sites followed by diffusion either through surface spillover or gas-phase diffusion to barium sites, and then stored as nitrates via disproportionation reaction ($BaO + 3NO_2 \rightarrow Ba(NO_3)_2 + NO$) with releasing a NO molecule. Both mechanisms are favored at an intimate contact between Pt and BaO. Noting that the Pt particles over the present catalysts were similar sized, lowering the Pt loading actually reduced the surface density of Pt particles, and resulted in smaller Pt–BaO contact boundary, which consequently led to the drop in NSC. Furthermore, the steeper NO curves (or NO_x curves) on lowering the Pt loading would also indicate that NO_x storage pathway is affected by the Pt loading. The steeper NO curves (or NO_x curves) mean that more NO slips the catalyst bed after NO_x breakthrough, which could be due to the additional NO formation via disproportionation reaction.

Table 1
Surface area, Pt dispersion, and composition of Pt–BaO/Al_2O_3, Pt–CoO_x–BaO/Al_2O_3 and Pt–BaO/ZrO_2–Al_2O_3 catalysts.

Catalysts	BET area (m^2/g-cat)	Pt dispersion (%)	Content (wt%)[a]		
			Pt	Ba	Co
1Pt–BaO/Al_2O_3	122	2.7[b] (2.9)[c]	0.97	15.2	–
0.5Pt–BaO/Al_2O_3	121	2.9 (3.0)	0.46	15.4	–
0.1Pt–BaO/Al_2O_3	116	3.1 (3.2)	0.13	15.0	–
0.5Pt–1CoO_x–BaO/Al_2O_3	109	(2.8)	0.46	15.3	0.98
0.5Pt–5CoO_x–BaO/Al_2O_3	82	(2.9)	0.44	15.2	4.91
0.5Pt–10CoO_x–BaO/Al_2O_3	69	(2.8)	0.47	15.5	9.94
1Pt–BaO/ZrO_2–Al_2O_3	125	2.7 (3.0)	0.95	15.6	–
0.5Pt–BaO/ZrO_2–Al_2O_3	126	2.9 (3.2)	0.45	15.3	–
0.1Pt–BaO/ZrO_2–Al_2O_3	124	3.3 (3.3)	0.12	15.3	–

[a] Determined by XRF.
[b] Measured by H_2–O_2 titration.
[c] Value in parentheses was obtained by using Scherer equation based on the diffraction of (1 1 1) plane at $2\theta = 39.8°$.

Table 2
NO_x storage and reduction performance measured under lean (1000 ppm NO, 10% O_2 in Ar)/rich (1% H_2 in Ar) conditions.

Catalyst	NO_x storage		NO_x reduction					
	NSC[a]	NO_2/NO_x[b] (%)	NRC[c]	Selectivity (N%)[d]				
				N_2	NH_3	N_2O	NO	NO_2
1Pt–BaO/Al_2O_3	0.27	58	0.23	84.5	14.4	1.1	–	–
0.5Pt–BaO/Al_2O_3	0.22	38	0.19	52.5	38.3	9.2	–	–
0.1Pt–BaO/Al_2O_3	0.13	16	0.11	15.6	66.5	17.9	–	–
0.5Pt–1CoO_x–BaO/Al_2O_3	0.24	43	0.12	49.2	45.0	5.8	–	–
0.5Pt–5CoO_x–BaO/Al_2O_3	0.25	75	0.13	51.3	39.5	4.9	4.3	–
0.5Pt–10CoO_x–BaO/Al_2O_3	0.41	93	0.14	29.8	19.7	24.2	23.4	2.9
1Pt–BaO/ZrO_2–Al_2O_3	0.28	69	0.25	87.1	8.2	4.7	–	–
0.5Pt–BaO/ZrO_2–Al_2O_3	0.25	48	0.21	84.8	9.3	5.9	–	–
0.1Pt–BaO/ZrO_2–Al_2O_3	0.13	21	0.12	65.6	28.1	6.3	–	–

[a] NO_x storage capacity (mmol/g-cat) based on nitrogen number under lean condition.
[b] NO_2 percentage in the effluent NO_x when the catalysts were saturated by NO/O_2 adsorption.
[c] Amount of N-containing species (mmol/g-cat) based on nitrogen number detected under rich condition.
[d] Time-averaged selectivity based on nitrogen number.

Therefore, the steeper NO curves on low platinum catalysts indicate that the "nitrate route" will prevail for catalysts with lower Pt loading or with smaller Pt–BaO contact boundary.

Fig. 2 shows the time-course during regeneration phase under the rich condition over Pt–BaO/Al_2O_3 catalysts. Upon admitting 1% H_2 to the reactor, no H_2 could be detected, and N_2 with a concentration about 2000 ppm appeared immediately for 1Pt–BaO/Al_2O_3 and 0.5Pt–BaO/Al_2O_3 catalysts. The value of around 2000 ppm agrees well with that expected from the stoichiometry of nitrates reduction with 1% H_2 ($2NO_3^- + 5H_2 \rightarrow N_2 + O^{2-} + 5H_2O$), indicating that the initial NO_x reduction is very fast and limited by the supply of H_2. The N_2 concentration on 0.1Pt–BaO/Al_2O_3, was much smaller (ca. 1000 ppm), which suggests that the reduction rate of the stored NO_x on the catalyst is much slower. The concentration of N_2 then decreased sharply to zero after keeping at high level for a certain period, coincident with the simultaneous evolution of H_2 and NH_3 in the effluent. The concentration of H_2 then quickly approached that (1%) of the inlet H_2, while the concentration of NH_3 quickly passed a maximum and tailed gradually to zero in the following 5–10 min. It should be noted that the area below the N_2 curve dropped significantly and that of NH_3 increased remarkably on lowering the Pt loading. N_2O was also detected at quite low level during the whole reduction phase.

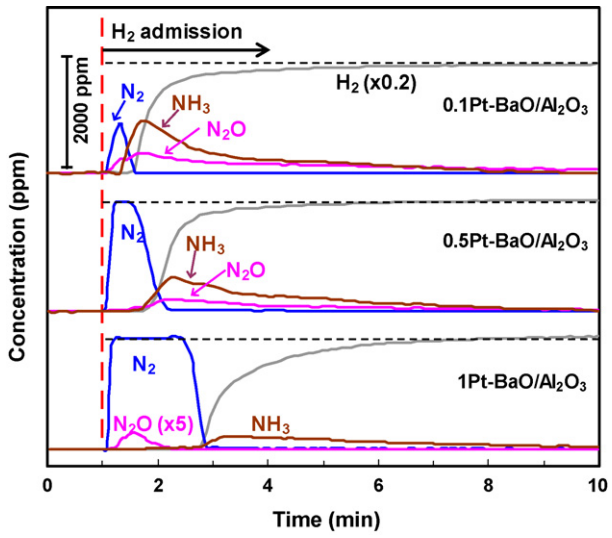

Fig. 2. Time-course during regeneration phase under the rich condition over Pt–BaO/Al_2O_3 catalysts with Pt loading of 1.0, 0.5 and 0.1 wt%, respectively.

These results reveal a shift of product from mainly N_2 to NH_3 during the reduction of the stored NO_x, which is in good agreement with the literature [12–15]. The time-averaged product selectivity during the rich regeneration condition is then obtained (Table 2). When the Pt loading on Pt–BaO/Al_2O_3 catalysts was reduced from 1.0 to 0.5 wt%, and to 0.1 wt%, the selectivity of N_2 decreased significantly from 85% to 53%, and to 16%, respectively, while the selectivity of NH_3 increased greatly from 14% to 38%, and to 67%, respectively. The amount of N-containing species (NRC) detected under the rich condition was above 85% of NSC. The difference between the NSC and NRC numbers is related to the amount of NO_x that are stored under the lean condition but cannot lead to NO_x abatement under the rich condition. This is largely due to that NO_x adsorption on Pt–BaO catalysts is an equilibrium-driven reaction [4,5,21] and some weakly adsorbed NO_x species was removed during the Ar purge intervening the lean/rich switches. Taking into account of the overall NO_x storage and reduction performance of Pt–BaO/Al_2O_3 catalysts, lowering the Pt loading from 1.0 to 0.1 wt% impacts more significantly on product selectivity during NO_x reduction under the rich condition than NO_x storage capacity under the lean condition. These results indicate that the NO_x reduction performance under the rich condition is the key to low platinum NSR catalysts.

3.3. *Promoting effect of CoO_x on the NSR performance of low platinum Pt–BaO/Al_2O_3*

The effect of CoO_x promotion on the NSR performance of low platinum Pt–BaO/Al_2O_3 was then studied by varying cobalt loading from 1 to 10 wt% in 0.5Pt–CoO_x–BaO/Al_2O_3 catalysts with 0.5 wt% Pt. Fig. 3 shows the time-course of NO_x storage under lean condition over these Pt–CoO_x–BaO/Al_2O_3 catalysts. Addition of CoO_x obviously prolonged the dead time for NO_x breakthrough, As a result, the NSC (Table 2) increased from 0.22 (0.5Pt–BaO/Al_2O_3) to 0.24 and 0.25 mmol/g for 0.5Pt–1CoO_x–BaO/Al_2O_3 and 0.5Pt–5CoO_x–BaO/Al_2O_3, respectively, and to 0.41 mmol/g when cobalt loading was 10 wt%. Moreover, the curves of NO_x after breakthrough became flatter on addition of CoO_x, and the NO_2 concentration after the catalysts being saturated with NO_x was also increased obviously: the NO_2/NO_x ratio increased from 0.38 for the CoO_x-free catalysts to 0.43, 0.75, and 0.93, respectively, when cobalt loading was 1.0, 5.0 and 10 wt%. These results are in line with the literature that CoO_x with strong oxidizing ability provides additional contact boundary for NO_x spillover to barium oxide sites [9,22].

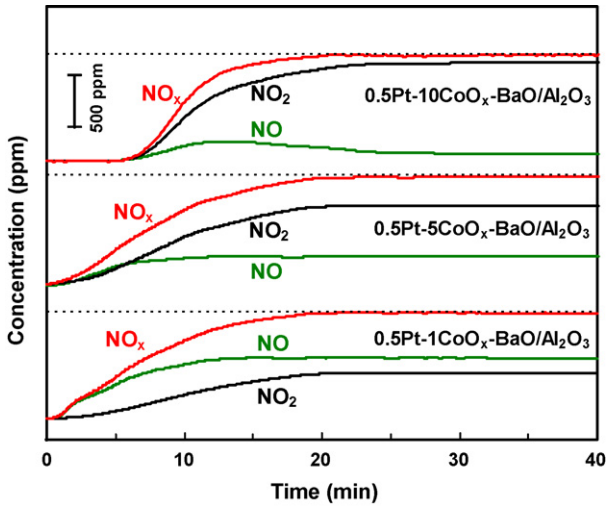

Fig. 3. Time-course of NO_x storage under the lean condition (breakthrough curve) over 0.5Pt–CoO_x–BaO/Al_2O_3 with varying cobalt loadings.

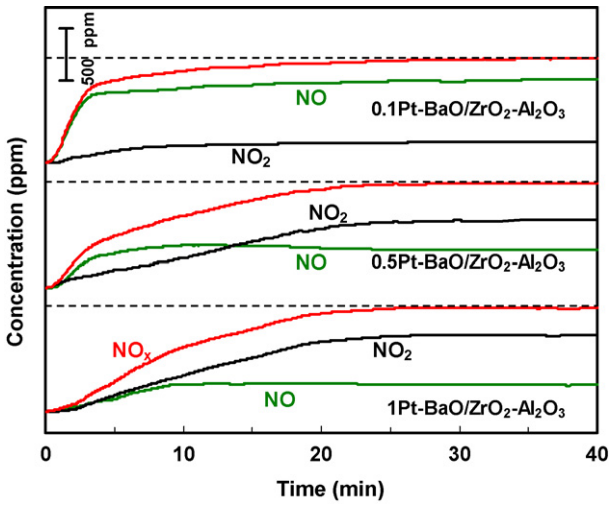

Fig. 5. Time-course of NO_x storage under the lean condition (breakthrough curve) over Pt–BaO/ZrO_2–Al_2O_3 catalysts with Pt loading of 1.0, 0.5 and 0.1 wt%, respectively.

For NO_x reduction under the rich condition (Fig. 4), complete consumption of H_2 was also observed at the initial stage. However, the maximum N_2 concentration as well as the area of N_2 decreased significantly on adding CoO_x to the low platinum Pt–BaO/Al_2O_3 catalyst. A shift of product from N_2 to NH_3 was observed for catalysts with cobalt loadings no higher than 5.0 wt%. For 0.5Pt–10CoO_x–BaO/Al_2O_3 catalyst with cobalt loading of 10 wt%, the formation of NH_3 was even detected at the initial stage of NO_x reduction. Furthermore, unreduced NO_x was clearly detected when cobalt loadings was 10 wt%. The quantified results (Table 2) showed that addition of CoO_x decreased the selectivity of N_2, and favored NH_3 formation on catalysts with cobalt loadings no higher than 5 wt%. For 0.5Pt–10CoO_x–BaO/Al_2O_3 catalyst, the N_2 selectivity was only 30%, which is due to the formation of N_2O and large amount of unconverted NO_x.

The numbers of NRC give more insight into the effect of CoO_x on NO_x reduction performance. The NRC decreased from 0.19 mmol/g for the reference 0.5Pt–BaO/Al_2O_3 to 0.12, 0.13 and 0.14 mmol/g for the catalysts with cobalt loadings of 1, 5 and 10 wt%, respectively. This results means that more than 50% of the stored NO_x over the CoO_x promoted catalysts has been removed during the Ar purge, which contrasts clearly with the retaining of around 86% of the stored NO_x over the reference 0.5Pt–BaO/Al_2O_3. Therefore, promoting low platinum Pt–BaO/Al_2O_3 with cobalt oxides severely deteriorated the NO_x reduction performance, indicating cobalt oxides are not suitable promoters for low platinum NSR catalysts.

3.4. Using ZrO_2–Al_2O_3 as an alternative of the Al_2O_3 support for low platinum Pt–BaO catalysts

The time-courses of NO_x storage and reduction under cyclic lean/rich conditions over Pt–BaO/ZrO_2–Al_2O_3 with Pt loading varying in 1.0–0.1 wt% are shown in Figs. 5 and 6, respectively. These curves are essentially similar to those of the reference Pt–BaO/Al_2O_3 with the similar Pt loadings: i.e., lowering the Pt loading reduced the dead time for NO_x breakthrough and resulted in steeper NO (or NO_x) curves after NO_x breakthrough under the

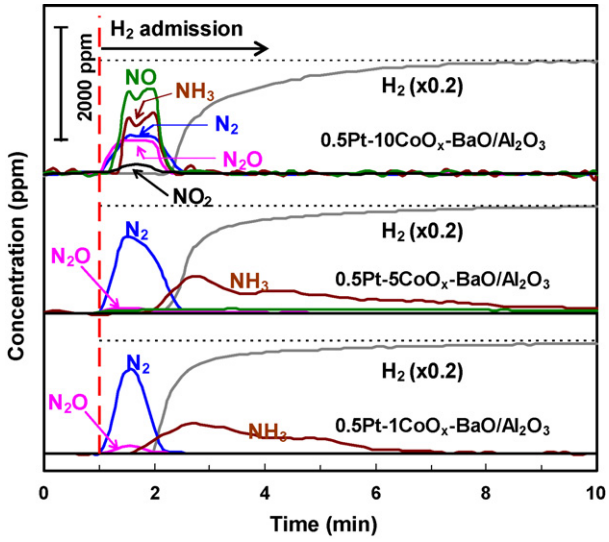

Fig. 4. Time-course during regeneration phase under the rich condition over 0.5Pt–CoO_x–BaO/Al_2O_3 with varying cobalt loadings.

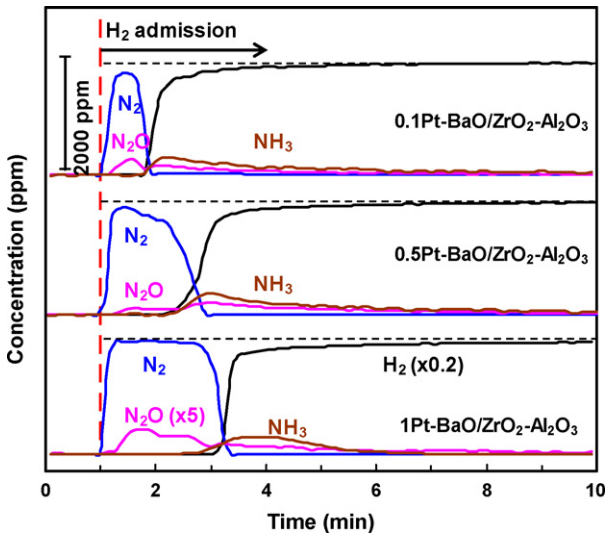

Fig. 6. Time-course during regeneration phase under the rich condition over Pt–BaO/ZrO_2–Al_2O_3 with Pt loading of 1.0, 0.5 and 0.1 wt%, respectively.

lean condition. The NSC over Pt–BaO/ZrO_2–Al_2O_3 was slightly larger than its counterpart Pt–BaO/Al_2O_3 with the similar Pt loading, which could be due to the higher oxidizing ability of Pt–BaO/ZrO_2–Al_2O_3 as manifested by the higher NO_2 percentages in effluent NO_x after the catalysts being saturated with the stored NO_x. However, both series of Pt–BaO/ZrO_2–Al_2O_3 and Pt–BaO/Al_2O_3 showed similar dependencies of NSC on the Pt loading (Table 2).

With regard to the NO_x reduction performance under the rich condition, a shift of product from mainly N_2 to NH_3 was also observed. The N_2 selectivity on 1.0Pt–BaO/ZrO_2–Al_2O_3 was slight larger than its Al_2O_3 supported counterpart. However, in contrast to the drastic decline of N_2 selectivity on lowering Pt loading in Pt–BaO/Al_2O_3, the N_2 selectivity on 0.5Pt–BaO/ZrO_2–Al_2O_3 with 0.5 wt% Pt remained at 84.8%. Even for 0.1Pt–BaO/ZrO_2–Al_2O_3, the N_2 selectivity was still 65.6% (Table 2). These numbers were significantly higher than those (53 and 16%) over the reference low platinum 0.5Pt–BaO/Al_2O_3 and 0.1Pt–BaO/Al_2O_3 catalysts. Formation of harmful NH_3 was greatly mitigated on low platinum Pt–BaO/ZrO_2–Al_2O_3 catalysts, which contrasts strongly with the drastic increase of NH_3 selectivity over Pt–BaO/Al_2O_3 catalysts on lowering the Pt loading. Clearly, using ZrO_2–Al_2O_3 as an alternative of the Al_2O_3 support for Pt–BaO catalysts effectively reduced the dependence on Pt loading of the Pt–BaO for the NSR catalysis since the ZrO_2–Al_2O_3 support could make the catalyst highly selective for the formation of N_2 under the rich condition. The overall NSR performance of a Pt–BaO/ZrO_2–Al_2O_3 catalyst with 0.5 wt% Pt was found comparable to that of Pt–BaO/Al_2O_3 catalyst with 1.0 wt% Pt.

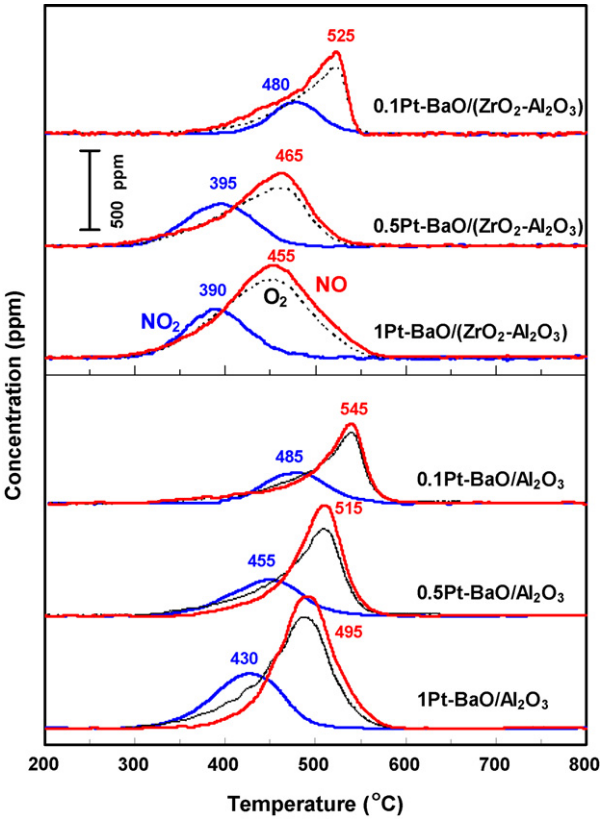

Fig. 7. NO_x-TPD profiles after saturating the catalysts with NO/O_2 adsorption.

3.5. Origins of the enhanced N_2 selectivity over low platinum Pt–BaO/ZrO_2–Al_2O_3 catalysts

The performance of NSR catalyst is controlled by a combination of the inherent differential catalytic performance and the integral nature of the catalyst in a "plug-flow" reactor. The catalyst regeneration phase under the rich condition, characterized by product shift from N_2 to NH_3, can be described by a moving down along catalyst bed of a reaction front, where reduction of the stored NO_x with H_2 generates various N-containing products (ca. NH_3, N_2O, N_2 and NO_x) and the formed NH_3 further reacts with the downstream nitrates to produce N_2 [12–15]. Therefore, the differential product selectivity at the reaction front could be largely reflected by their temporal evolution at the end of NO_x reduction when the reaction front moves to the bottom of the catalyst bed. Thus, the enhanced N_2 selectivity over Pt–BaO/ZrO_2–Al_2O_3 catalysts is actually due to the higher differential selectivity of N_2 (or lower NH_3 selectivity) at the reaction front.

Various mechanisms regarding the reduction of the stored NO_x at the reaction front have been proposed [4,12–15,23], and the differential product selectivity at the reaction front is critically dependent on the NO_x/H_2 ratio over Pt sites that were generally assumed to be the active sites for NO_x reduction. The availability of NO_x at Pt sites, i.e., the release of NO_x from the trapping barium sites to Pt sites, is therefore crucial to the product selectivity under the rich condition. The NO_x release performance was then evaluated by NO_x-TPD (Fig. 7) after saturating these catalysts with NO/O_2 adsorption in cycle-average steady state. All the NO_x-TPD curves were characterized by two NO_x desorption peaks: desorption of NO_2 with a small amount of O_2 at relatively lower temperatures, and of NO with relatively large amount of O_2 at higher temperatures, which could be attributed to the decomposition of surface and "bulk-like" barium nitrates species, respectively [24,25]. The amount of desorbed NO_x in NO_x-TPD was found comparable to that adsorbed during cyclic lean-rich conditions. However, both the desorption temperatures of NO_2 and NO were parallelly shifted on lowering the Pt loading. For Pt–BaO/Al_2O_3 catalysts, decreasing Pt loading from 1.0 to 0.5 wt%, and to 0.1 wt% apparently increased the peak temperatures for NO desorption from 495 to 515 and to 545 °C, respectively. On the other hand, NO_x desorption from Pt–BaO/ZrO_2–Al_2O_3 occurred at much lower temperatures than their Al_2O_3 supported counterparts. Moreover, the desorption temperature from Pt–BaO/ZrO_2–Al_2O_3 was nearly not affected when Pt loading was decreased from 1.0 to 0.5 wt%. (NO desorption temperature was 455 and 465 °C, respectively, for the catalysts with Pt loadings of 1.0 and 0.5 wt%.) Only after the Pt loading was decreased to 0.1 wt%, considerable increases in NO_x desorption temperature (525 °C) were observed. Clearly, replacing Al_2O_3 with ZrO_2–Al_2O_3 de-stabilized the stored NO_x on Pt–BaO catalysts and also reduced the dependence of NO_x desorption temperature on Pt loading.

The stability of the stored NO_x, as indicated by the NO desorption temperature in NO_x-TPD experiment, was then correlated with the selectivities of N_2 and NH_3 under the rich condition (Fig. 8). The strong dependencies clearly show that the lower the desorption temperature of NO (the lower stability of the stored NO_x), the higher the N_2 selectivity, or the lower the NH_3 selectivity. Therefore, it can be concluded that the relatively lower stability of the stored NO_x on Pt–BaO/ZrO_2–Al_2O_3 catalysts improved the availability of NO_x at the Pt sites, and remarkably enhanced the N_2 selectivity.

The oxidative adsorption of NO_x on Pt–BaO catalysts is an equilibrium-driven reaction [4,5,20,23]. According to the principle of micro-reversibility, the redox properties of Pt would impact on the stability of the stored NO_x. To gain insight into the cause for the destabilizing effect of ZrO_2–Al_2O_3 support on the stored NO_x, the redox properties of 0.5Pt–BaO/Al_2O_3 and 0.5Pt–BaO/ZrO_2–Al_2O_3 catalysts were compared.

Fig. 9 shows the H_2-TPR curves of 0.5Pt–BaO/ZrO_2–Al_2O_3 and 0.5Pt–BaO/Al_2O_3 catalysts. Both catalysts exhibited weak H_2 con-

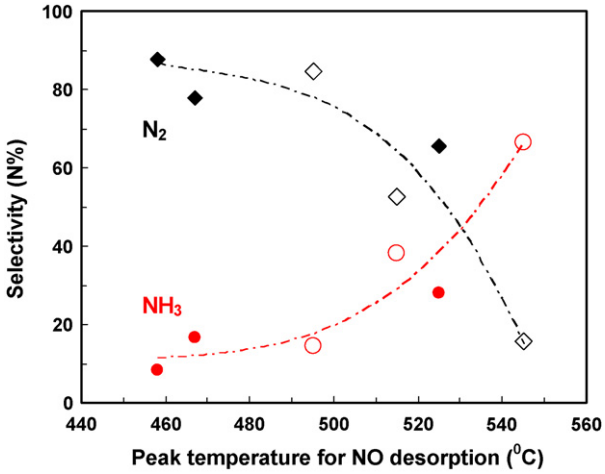

Fig. 8. Correlations between the NO desorption temperature in NO_x-TPD experiment and the selectivities of N_2 (♦◊) and NH_3 (●○) under regeneration phase. Closed signals: data of Pt–BaO/ZrO_2–Al_2O_3 catalysts; open signals: data of Pt–BaO/Al_2O_3 catalysts.

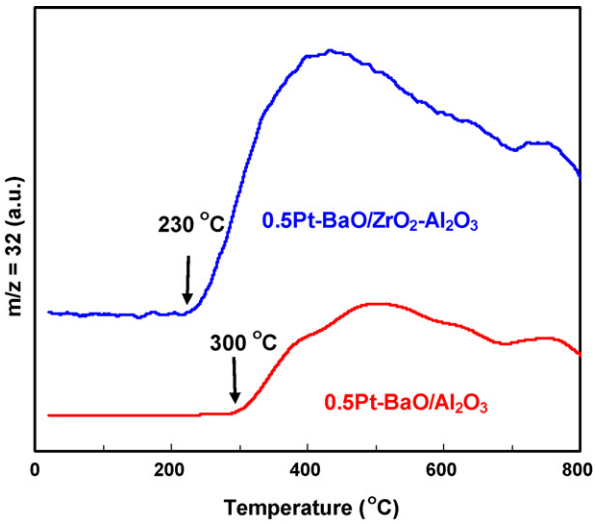

Fig. 10. O_2-TPD profiles of ZrO_2–Al_2O_3 and Al_2O_3 supported 0.5Pt–BaO catalysts.

sumption peaks below 500 °C, due to the reduction of oxygen adsorbed on metallic Pt particles or of surface PtO_x species [26], and strong H_2 consumption peaks around 700 °C due to the Pt-promoted reduction of Al_2O_3 and/or ZrO_2. 0.5Pt–BaO/ZrO_2–Al_2O_3 catalyst produced sharp peak at 160 °C and broad peak at 370 °C, while very weak peak at 230 °C and broad peak at 380 °C were detected over 0.5Pt–BaO/Al_2O_3. The O_2-TPD profiles of the two catalysts were compared in Fig. 10. The onset temperature for O_2 desorption from 0.5Pt–BaO/ZrO_2–Al_2O_3 was 230 °C, much lower than that (300 °C) for Al_2O_3 supported counterpart. Noting that the metallic Pt particles were similarly sized in these samples (Table 1), the results of H_2-TPR and O_2-TPD thus clearly indicate that ZrO_2–Al_2O_3 support induces a weaker O–Pt interaction than Al_2O_3 support. The easier removal of the surface oxygen adsorbed on Pt in Pt–BaO/ZrO_2–Al_2O_3 catalysts would create a driving force for oxygen atoms migration from the barium sites to Pt, thus destabilizing the stored nitrates [23]. And consequently improves the availability of NO_x on Pt and leads to higher N_2 selectivity. The weaker oxygen adsorption on Pt–BaO/ZrO_2–Al_2O_3 catalysts also nicely explains their higher oxidation ability under lean condition, since blocking of Pt sites by strongly adsorbed oxygen has been recognized as the main reason for the catalyst deactivation during NO oxidation [27].

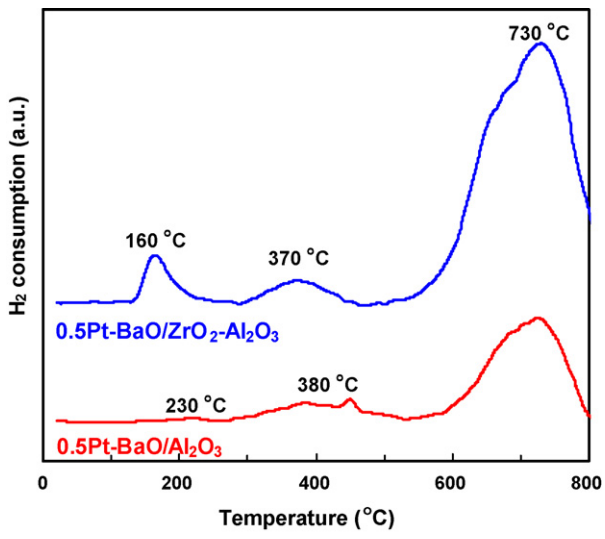

Fig. 9. H_2-TPR profiles of ZrO_2–Al_2O_3 and Al_2O_3 supported 0.5Pt–BaO catalysts.

4. Conclusions

This work showed a strong dependency of the NSR catalysis on Pt loading of the reference Pt–BaO/Al_2O_3 catalyst. Efficient NO_x reduction catalysis under the rich condition is the key to developing innovative low platinum NSR catalysts. The cobalt oxides appeared to be an unsuitable promoter for lowering the Pt loading as its addition into the Pt–BaO/Al_2O_3 catalyst would significantly reduce the N_2 selectivity under the rich condition. It was found that the use of ZrO_2–Al_2O_3 as an alternative of the Al_2O_3 support was effective in lowering the dependence on Pt loading of the Pt–BaO for the NSR catalysis since the ZrO_2–Al_2O_3 support could make, at a lower Pt loading, the catalyst highly selective for the formation of N_2 under the rich condition. This finding provides a viable approach in the search for low platinum NSR catalysts.

Acknowledgements

We acknowledge the financial support from the NSF of China (Grants: 20703028 and 20921001) and China Postdoctoral Science Foundation (Grant: 20070420350).

References

[1] R. Burch, Catal. Rev. 46 (2004) 271.
[2] N. Miyoshi, S. Matsumoto, K. Katoh, T. Tanaka, J. Harada, N. Takahashi, K. Ypkota, M. Sugirura, K. Kasahara, SAE Tech. Paper 950809, 1995.
[3] S. Matsumoto, CATTECH 4 (2000) 102.
[4] W.S. Epling, L.E. Campbell, A. Yezerets, N.W. Currier, J.E. Parks, Catal. Rev. 46 (2004) 163.
[5] S. Roy, A. Baiker, Chem. Rev. 109 (2009) 4054.
[6] J.M. Trichard, Stud. Surf. Sci. Catal. 171 (2007) 212.
[7] Y. Liu, M. Meng, X.G. Li, L.H. Guo, Y.Q. Zha, Chem. Eng. Res. Des. 86 (2008) 932.
[8] N. Takahashi, A. Suda, I. Hachisuka, M. Sugiura, H. Sobukawa, H. Shinjoh, Appl. Catal. B: Environ. 72 (2006) 187.
[9] R. Vijay, C.M. Snively, J. Lauterbach, J. Catal. 243 (2006) 368.
[10] Y. Ji, J.-S. Choi, T.J. Toops, M. Crocker, M. Naseri, Catal. Today 136 (2008) 146.
[11] P.N. Lê, E.C. Corbos, X. Coutois, F. Can, S. Royer, P. Marecot, D. Duprez, Top. Catal. (2009), doi:10.1007/s11244-009-9345-7.
[12] L. Lietti, I. Nova, P. Forzatti, J. Catal. 270 (2008) 257.
[13] S.S. Mulla, S.S. Chaugule, A. Yezerets, N.W. Currier, W.N. Delagass, F.H. Ribeiro, Catal. Today 136 (2008) 136.
[14] I. Nova, L. Castoldi, L. Lietti, E. Tronconi, P. Forzatti, Top. Catal. 42–43 (2007) 21.
[15] W.S. Epling, A. Yezerets, N.W. Currier, Appl. Catal. B: Environ. 74 (2007) 117.
[16] B.-Q. Xu, J.-M. Wei, H.-Y. Wang, K.-Q. Sun, Q.-M. Zhu, Catal. Today 68 (2001) 217.

[17] D.H. Kim, Y.H. Chin, G.G. Muntean, A. Yezeretz, N.W. Currier, W.S. Epling, H.-Y. Chen, H. Hess, C.H.F. Peden, Ind. Eng. Chem. Res. 45 (2006) 8815.
[18] J. Dawody, L. Eurenius, H. Abdulhamid, M. Skoglundh, E. Olsson, E. Fridell, Appl. Catal. A: Gen. 296 (2005) 157.
[19] I. Nova, L. Castoldi, L. Lietti, E. Tronconi, P. Forzatti, Catal. Today 75 (2002) 431.
[20] T.J. Toops, B.G. Bunting, K. Nguyen, A. Gopinath, Catal. Today 123 (2007) 285.
[21] J. Coronado, J. Anderson, J. Mol. Catal. A: Chem. 138 (1999) 83.
[22] R. Vijay, H. Sakurai, C.M. Snively, J. Lauterbach, Top. Catal. 52 (2009) 1388.
[23] P. Forzatti, L. Lietti, I. Nova, Energy Environ. Sci. 1 (2008) 236.
[24] N.W. Cant, M.J. Patterson, Catal. Today 73 (2002) 271.
[25] T. Szailer, J.H. Kwak, D.H. Kim, J. Szanyi, C.M. Wang, C.H.F. Peden, Catal. Today 114 (2006) 86.
[26] K.S. Karbin, P. Khanna, R.L. Muncrief, V. Medhekar, M.P. Harold, Catal. Today 114 (2006) 72.
[27] L. Olsson, E. Fridell, J. Catal. 210 (2002) 340.